Constraint Screening for Security Analysis of Power Networks

Ramtin Madani, Javad Lavaei and Ross Baldick

***Abstract*—Consider a general security-constrained unit commitment (SCUC) problem for an arbitrary power network. This problem includes discrete variables corresponding to commitment parameters as well as demand and generation constraints, among others. Aside from its non-convexity, SCUC is a large-scale problem for real-world systems due to the security constraints. The main objective of this paper is to propose an algorithm to eliminate a vast majority of linear security constraints in the high-dimensional mixed-integer SCUC problem in order to arrive at an equivalent reduced-order SCUC problem. To this end, we develop a parallel and computationally cheap algorithm for finding a minimal subset of security constraints whose satisfaction guarantees the satisfaction of all security constraints. The proposed algorithm does not depend on the unknown unit commitment parameters and allows the load forecasts to be imprecise. More specifically, a low-order model of the SCUC problem is found based on the topology of the power system, given lower and upper bounds on nodal power injections (to accommodate uncertainties in loads and generation productions), and the normal and emergency line ratings. This algorithm is tested on several power systems with as many as 5500 buses, for which each set of security constraints with millions of conditions is reduced to a minimal subset with only a few hundred conditions.**

I. Introduction

Security analysis is an important aspect of both planning and real-time operation of power networks. A modern grid consists of a large number of components such as generators, transmission lines, transformers, phase shifters and other power electronic devices. Each power component is subject to a possible outage with some probability and its failure affects the operation of other devices in the network [1], [2]. A main job of the system operator is to ensure that the demand, network, physical, and technological constraints are all met satisfactorily under certain failure scenarios, named *contingency cases*. If not controlled appropriately, a failure could lead to a catastrophic event and impact the economy; examples include major blackouts caused by cascading failures in power grids [3], [4].

An extensive list of contingency cases is considered in practice, along with a set of instantaneous and delayed corrective actions associated with each case. In order to return to a normal operating condition in case of a contingency, corrective actions should be taken within specific time intervals. Although major demand and technical constraints should be met at all times, minor violations of certain constraints are permitted for a short period of time. For example, each transmission line usually has multiple flow limits, referred to as *short-term and long-term limits* or *normal and emergency ratings*, where emergency ratings are higher than normal ratings. These limits depend on the contingency time frame and the pre-contingency operating point, and are obtained based on the fact that the line temperature depends on not only the magnitude of the current but also the period over which the current has flowed in the line [5]. In other words, the limits imposed on each component of the network during a contingency are often less restrictive than those for the pre-contingency condition of the component.

The real-time operation of power grids requires solving a fundamental optimization problem with a large number of continuous and discrete variables subject to market and technical constraints. This problem is referred to as the security-constrained unit commitment (SCUC) problem. The large number of constraints associated with different contingency cases poses an important challenge for solving the mixed-integer SCUC problem. Although the number of security constraints is theoretically prohibitive, empirical evidence shows that a vast majority of the constraints are redundant and only a small subset of constraints could be binding regardless of the load profiles [6]. A well-known bounding technique, for example, has long been used in order to obtain a set of potentially binding constraints [7], [8]. The recent papers [9] and [10] have also studied the problem of identifying redundant security or flow constraints. The common practice in the power industry includes an iterative procedure, where each iteration involves the following steps: solving the unit commitment problem with a smaller set of constraints, testing the possible violation of ignored constraints, adding some of the violated constraints to the problem, and then resolving the modified problem in the next iteration [11], [12]. The violation test is conducted through modules that are commonly regarded as Network Security Monitoring (NSM) and Simultaneous Feasibility Testing (SFT) [5], [13].

Such an iterative procedure, however, can be computationally expensive and unnecessarily time consuming. A question arises as to whether the performance of this procedure can be improved dramatically. Motivated by the above-mentioned challenges, this work is concerned with the identification of a minimal set of potentially binding constraints prior to solving the SCUC problem. In order to identify the redundant constraints, we adopt an optimization-based bound tightening scheme that relies on solving a collection of simple linear programs in parallel, which obtains lower and upper bounds on each scalar parameter of the pre-contingency network. An interval arithmetic procedure can then be executed in order to declare redundancies based on the calculated bounds [14], [15]. More precisely, the proposed algorithm first obtains a

Ramtin Madani is with the Electrical Engineering Department at the University of Texas at Arlington (ramtin.madani@uta.edu). Javad Lavaei is with the Department of Industrial Engineering and Operations Research, University of California, Berkeley (lavaei@berkeley.edu). Ross Baldick is with the Department of Electrical and Computer Engineering, University of Texas at Austin (baldick@ece.utexas.edu). This work was supported by ONR YIP Award, DARPA Young Faculty Award, NSF CAREER Award 1351279, and NSF EECS Awards 1406894 and 1406865.

hypercube containing the feasible set and then cancels the constraints that do not intersect with the hypercube. Each bound tightening linear program is solved subject to a modest number of constraints as opposed to the entire set of security constraints, with the aim of making the calculation of bounds efficient. We have observed through extensive simulations on real-world networks that the proposed algorithm is able to declare more than 99.99% of the constraints as redundant.

Bound tightening algorithms have become an important part of the preprocessing step for mixed-integer programming (MIP) solvers. The main objectives of bound tightening include: strengthening convex relaxations, reducing the size of the domain over which enumeration is performed, and facilitating the identification of redundant constraints. Optimization-based bound tightening offers lower and upper bounds on each variable by minimizing and maximizing the variable over a relaxed feasible region [16]–[19]. Although solving two optimization problems for every scalar parameter of MIP can be expensive, we adopt efficient choices for the relaxed feasible sets in order to reduce the computational burden. In addition, we analyze an alternative approach from [20] for obtaining easy-to-calculate lower and upper bounds, which is shown to be capable of eliminating a large portion of constraints in our experiments.

Interval arithmetic methods and bound tightening approaches have been previously applied to power system analysis [21], as well as contingency analysis [12], and in particular SCUC under uncertainty [22], [23]. In [23], an interval optimization approach is adopted in order to accommodate uncertainty of wind generation for unit commitment. A scenario reduction procedure is introduced in [23], through which generator commitments are bounded and redundant nodal injection scenarios are canceled accordingly. Through a Benders' cut decomposition scheme, the UC problem under study is broken down into smaller subproblems associated with the remaining scenarios. Moreover, certain necessary conditions are developed in [22] in order to diagnose line congestions during ramping, prior to solving UC. The paper [12] offers a novel formulation by means of shift factor coefficients that captures a variety of practical considerations such as transmission contingency and wind uncertainty. Our work is related to the recent papers [6] and [24], which offer mathematically-rigorous integer programming schemes for the elimination of redundant constraints. However, the above-mentioned methods suffer from scalability issues as well as restrictive assumptions, and the simulations performed in those papers are limited to small-sized systems. For instance, contingency cases are not considered in [23] and [22], and the method proposed in [12] is only guaranteed to remain robust to contingencies if the wind is realized at the expected level. In contrast, the method proposed in this paper is designed to handle real-world systems and ranges of generation and load. The computational method developed in this work analyzes those security constraints of the problem that are modeled linearly with respect to the base-case parameters.

The rest of this paper is organized as follows: Section II describes the modeling and formulation of the problem. Section III develops a constraint screening algorithm. Section IV offers simulation results on real-world systems, followed by conclusions in Section V.

A. Notations

The symbol $\mathbb{R}$ denotes the set of real numbers. Matrices are shown by capital and bold letters. The symbol $(\cdot)^{\mathrm{T}}$ denotes the transpose operator. $\mathrm{diag}\{\mathbf{A}\}$ denotes the diagonal vector of the square matrix $\mathbf{A}$. For two vectors $\mathbf{v}$ and $\mathbf{u}$ of the same dimension, $\mathbf{u} \leq \mathbf{v}$ means that every entry of $\mathbf{u}$ is less than or equal to the corresponding entry of $\mathbf{v}$. The (i, j) entry of $\mathbf{A}$ is denoted as A_{ij}. The notation $|\cdot|$ denotes the entry-wise absolute value. The $k \times k$ identity matrix is denoted as $\mathbf{I}_{k\times k}$. The standard basis for $\mathbb{R}^n$ is denoted by $\mathbf{e}_1, \mathbf{e}_2, \ldots, \mathbf{e}_n$. For a statement q, the notation $\mathcal{I}_q$ is reserved for the indicator function that takes the value 1 if q is true and 0 otherwise.

II. Problem Formulation and Modeling

Consider a security-constrained unit commitment problem with continuous and discrete variables, as well as linear and nonlinear constraints. This problem can be formulated as (see [11]):

$$\begin{aligned}
&\underset{\substack{\mathbf{y}\in\mathbb{R}^{n_y}\\ \mathbf{z}\in\mathcal{F}}}{\text{minimize}} && h_0(\mathbf{y},\mathbf{z}) && && \text{(1a)}\\
&\text{subject to} && h_i(\mathbf{y},\mathbf{z}) = 0 && i = 1,\ldots,m' && \text{(1b)}\\
& && h_i(\mathbf{y},\mathbf{z}) \leq 0 && i = m'+1,\ldots,m && \text{(1c)}\\
& && \mathbf{B}\mathbf{y} \leq \mathbf{a}. && && \text{(1d)}
\end{aligned}$$

The variables $\mathbf{y} = (\mathbf{y}_1, \mathbf{y}_2, \ldots, \mathbf{y}_{t'}) \in \mathbb{R}^{n_y}$ and $\mathbf{z} \in \mathcal{F}$ consist of continuous and discrete system parameters over the time horizon $t = 1, 2, \ldots, t'$, respectively, where

- The vector $\mathbf{y}_t$ is the set of continuous parameters at time $t \in \{1, 2, \ldots, t'\}$ (e.g., power injections and line flows).
- The vector $\mathbf{z}$ contains all discrete variables of the problem such as the on/off status of generators and lines.
- $\mathcal{F} \subseteq \mathbb{R}^{n_z}$ is an arbitrary feasible set for the vector $\mathbf{z}$. For example, this set could encode the integrality requirement of the commitment variables.

For every $i = 1, \ldots, m$, the function $h_i(\cdot,\cdot) : \mathbb{R}^{n_y} \times \mathbb{R}^{n_z} \to \mathbb{R}$ is assumed to be arbitrary and accounts for network, physical, technological and nonlinear reliability constraints, among others. In contrast, the linear constraints with respect to $\mathbf{y}$ are given in (1d), for known matrices $\mathbf{B} \in \mathbb{R}^{n_a\times n_y}$ and $\mathbf{a} \in \mathbb{R}^{n_a}$. The cost function $h_0(\cdot,\cdot)$ is also arbitrary.

There are pre-specified failure scenarios corresponding to each time period. If any of these scenarios takes place, system operators need to ensure that the lines of the system will not be overheated and that the demand at important buses will still be met. Define the *base case* (pre-contingency) of the network as the normal operating scenario, where no fault has happened and all of the committed generators, loads and lines are in service. Our primary assumption in this work is that the network equations are linearized in order to model most of the contingencies. More precisely, similar to many prior papers such as [25] and [11], we assume that, to a reasonable level of approximation, security constraints associated with a time period $t \in \{1, 2, \ldots, t'\}$ can be estimated as linear constraints in the form:

$$\mathbf{B}_t \, \mathbf{y}_t \leq \mathbf{a}_t, \tag{2}$$

which can then be captured by (1d). We will later demonstrate through multiple examples that a variety of contingency cases can be modeled linearly with respect to the base case parameters, under some technical assumptions.

While the presence of nonlinear constraints and discrete parameters contributes to the computational complexity, one major challenge for solving (1) is the extensive number of linear security constraints for the models used by independent system operators. The objective of this paper is to introduce an efficient model reduction algorithm to identify redundant linear security constraints associated with different time periods (based on a linear approximation of power flow equations). The goal is to obtain a reduced-order model of the linear security constraints. The proposed algorithm accommodates uncertainties in load profiles and does not require any knowledge of the unit commitment solutions, the cost function $h_0(\cdot, \cdot)$ and the nonlinear constraints of the problem.

A. Terminology

Suppose that the power system under study has n_b buses, n_g generators, n_d loads, and n_l branches. The analysis to be provided in this paper can be applied to each time instance $t_0 \in \{1, 2, ..., t'\}$ separately. Consider a time instance t_0, and define d_r as the amount of active power consumed by the load $r \in \{1, \ldots, n_d\}$ and g_s as the amount of active power produced by the generator $s \in \{1, \ldots, n_g\}$ at time t_0. Assume that the network is lossless and, therefore, each line can be characterized by a single flow as opposed to two flows at each end. Hence, we orient the lines of the network arbitrarily and define f_q as the power flow over the directed line $q \in \{1, \ldots, n_l\}$. Let $n \triangleq n_g + n_d + n_l$, and define

$$\mathbf{x} \triangleq [\, \mathbf{g}^{\mathrm{T}} \quad \mathbf{d}^{\mathrm{T}} \quad \mathbf{f}^{\mathrm{T}} \,]^{\mathrm{T}} \in \mathbb{R}^n$$

to be a vector representing the base-case operating point of the system, where

$$\mathbf{g} \triangleq [g_s]_{s=1}^{n_g}, \quad \mathbf{d} \triangleq [d_r]_{r=1}^{n_d} \quad \text{and} \quad \mathbf{f} \triangleq [f_q]_{q=1}^{n_l}$$

are the power generation, demand and flow vectors, respectively. Note that $\mathbf{x}$ plays the role of $\mathbf{y}_{t_0}$.

Throughout the paper, we assume that the on/off status of generators, the amount of power produced at each bus and the exact load values may be unknown. The only available information is lower and upper limits for each entry of $\mathbf{x}$, which reflect physical and technological constraints as well as the possibly uncertain forecast of the demand at time t_0. To formulate this, define

$$\mathbf{l} \in (\mathbb{R} \cup \{-\infty\})^n \quad \text{and} \quad \mathbf{u} \in (\mathbb{R} \cup \{+\infty\})^n$$

to be the lower and upper bound vectors for $\mathbf{x}$ such that the inequalities

$$\mathbf{l} \leq \mathbf{x} \leq \mathbf{u} \tag{3}$$

encapsulate all base-case conditions on the individual components, including the capacity of each generator, demand predictions, and long-term line ratings.

Multiple loads and generators can be connected to a single bus. Define the incidence matrices $\mathbf{D} \in \{0, 1\}^{n_b \times n_d}$ and $\mathbf{G} \in \{0, 1\}^{n_b \times n_g}$ such that $D_{ir} = 1$ if and only if the load r is at bus i and $G_{is} = 1$ if and only if the generator s is at bus i. Then, the nodal power injection vector $\mathbf{p} \in \mathbb{R}^{n_b}$ can be defined in terms of $\mathbf{g}$ and $\mathbf{d}$ through the formula

$$\mathbf{p} \triangleq \mathbf{G}\mathbf{g} - \mathbf{D}\mathbf{d} \tag{4}$$

B. Linearization of Network Equations

For real-time operations, it is a common practice to obtain a nominal base-case operating point $\hat{\mathbf{x}}$ by solving a nonlinear AC power flow problem. The nominal point $\hat{\mathbf{x}}$ can then be adopted as the point around which the linearization of the power balance equations is performed. In this case, reactive power flows and injections can also be included among the network parameters.

For many applications, however, the DC modeling of power systems can be adopted in which the voltage magnitudes are all assumed to be 1 per unit, each branch is modeled as a series inductor, and the phase angle difference across each line is assumed to be relatively small. Under the DC modeling, the changes of line flows with respect to the perturbations of the real power injections can be described by the sensitivity formula

$$\Delta\mathbf{f} = \mathbf{H}\Delta\mathbf{p}, \tag{5}$$

where $\mathbf{H} \in \mathbb{R}^{n_l \times n_b}$ is the power transfer distribution factor (PTDF) matrix for the base case network [26]. Therefore, the network equations can be represented in terms of $\mathbf{x}$ as

$$\mathbf{A}\mathbf{x} = \mathbf{b}, \tag{6}$$

where

$$\mathbf{A} \triangleq \begin{bmatrix} \mathbf{H}\mathbf{G} & -\mathbf{H}\mathbf{D} & -\mathbf{I}_{n_l \times n_l} \end{bmatrix} \tag{7}$$

and $\mathbf{b} \in \mathbb{R}^n$ corresponds to non-passive components in the network such as phase shifters.

The formulation given in (1) accepts both linear and nonlinear contingency constraints. As a common practice in the power industry, most of contingency constraints are modeled based on approximate linear relations between the pre- and post-contingency operation states. As illustrated in the next section, this assumption is met for common contingency scenarios under both preventive control and corrective control (such as transmission switching or the use of fast-ramping generators as a recourse action), provided that the network equations are linear. This is simply due to the linearization of power flow equations and the fact that most corrective actions in case of a contingency are simple policies (designed offline) that satisfy the superposition property. Although we adopt a DC model, it is possible to include reactive power and power losses in the model by considering the flows in both directions of each line in the state vector $\mathbf{x}$ and linearizing the network equations around a point that corresponds to nonzero voltage angles. The objective of this work is to eliminate the redundant linear security constraints, even in presence of possibly nonlinear power flow equations for the base case and arbitrary nonlinear security constraints in (1b) and (1c). However, the underlying assumption is that most of the security constraints are linear (as opposed to nonlinear), and therefore it is beneficial to preprocess them and find a reduced-order model.

C. Outages

Under the DC modeling assumption, suppose that there are n_c post-contingency cases, each involving the outage of an arbitrary combination of generators, loads, and branches. Let $\mathbf{x}^{(k)} \in \mathbb{R}^n$ denote the post-contingency operating point corresponding to the case $k \in \{0, 1, \ldots, n_c\}$. Define $\mathbf{l}^{(k)}$ and $\mathbf{u}^{(k)}$ as the (normal or emergency) lower and upper bounds for $\mathbf{x}^{(k)}$, where $k = 0$ represents the base case scenario, i.e.,

$$\mathbf{l}^{(0)} = \mathbf{l}, \quad \mathbf{u}^{(0)} = \mathbf{u} \quad \text{and} \quad \mathbf{x}^{(0)} = \mathbf{x}.$$

Therefore, the pre- and post-contingency constraints of the network are as follows:

$$\mathbf{l}^{(k)} \leq \mathbf{x}^{(k)} \leq \mathbf{u}^{(k)}, \qquad k = 0, 1 \ldots, n_c. \tag{8}$$

In this paper, we consider a linear interrelation among the pre- and post-contingency operating points. More precisely, we assume that

$$\mathbf{x}^{(k)} = \mathbf{F}^{(k)} \mathbf{x} \tag{9}$$

for every $k \in \{0, 1, \ldots, n_c\}$, where $\mathbf{F}^{(k)} \in \mathbb{R}^{n \times n}$ is a given matrix associated with the operating case k. A large variety of contingencies can be modeled through the equation (9) under linearity assumptions. In order to illustrate this, four simple examples for the simple 9-bus network depicted in Figure 1(a) will be provided below.

Example 1 (Line outage)**.** *Consider the outage of branches* 1 *and* 4*. Suppose that the outage does not affect the power injection vectors, i.e.,*

$$\mathbf{p}^{(1)} = \mathbf{p}^{(0)}. \tag{10}$$

Given the assumption (10)*, this contingency can be modeled using a Generalized Linear Outage Distribution Factor (GLODF) matrix* $\mathbf{O} \in \mathbb{R}^{n_l \times 2}$ *as*

$$\mathbf{f}^{(1)} = \mathbf{f}^{(0)} + \mathbf{O} \begin{bmatrix} f_1^{(0)} \\ f_4^{(0)} \end{bmatrix} \tag{11}$$

(see [27]). Therefore, we have a linear interrelation between $\mathbf{x}^{(0)}$ *and* $\mathbf{x}^{(1)}$ *in the form of* (9)*, where*

$$\mathbf{F}^{(1)} = \left[\begin{array}{c|c|c} \mathbf{I}_{n_g \times n_g} & \mathbf{0}_{n_g \times n_d} & \mathbf{0}_{n_g \times n_l} \\ \hline \mathbf{0}_{n_d \times n_g} & \mathbf{I}_{n_d \times n_d} & \mathbf{0}_{n_d \times n_l} \\ \hline \mathbf{0}_{n_l \times n_g} & \mathbf{0}_{n_l \times n_d} & \mathbf{I}_{n_l \times n_l} + \mathbf{O} \left[\tilde{\mathbf{e}}_1 \quad \tilde{\mathbf{e}}_4\right]^{\mathrm{T}} \end{array}\right]$$

and $\tilde{\mathbf{e}}_1, \tilde{\mathbf{e}}_2, \ldots, \tilde{\mathbf{e}}_{n_l}$ *denote the standard basis for* $\mathbb{R}^{n_l}$*.*

Example 2 (Generator outage)**.** *Consider the outage of generators* 1 *and* 4*. In order to preserve the network balance, it is a common practice to assume that the amount of power production for contingent generators would be distributed among in-service generators after the outage, proportional to their maximum capacity [26]. In other words, we can consider a custom proportionality factor matrix* $\mathbf{Q} \in \mathbb{R}^{n_g \times 2}$ *such that*

$$\mathbf{g}^{(2)} = \mathbf{g}^{(0)} + \mathbf{Q} \begin{bmatrix} g_1^{(0)} \\ g_4^{(0)} \end{bmatrix}, \tag{12}$$

where

$$Q_{11} = -1, \quad Q_{12} = 0, \quad Q_{42} = -1, \quad Q_{41} = 0 \tag{13}$$

and

$$\sum_{i=1}^{n_g} Q_{i1} = \sum_{i=1}^{n_g} Q_{i2} = 0. \tag{14}$$

Then, according to (5)*, we have:*

$$\mathbf{f}^{(2)} = \mathbf{f}^{(0)} + \mathbf{H}\mathbf{Q} \begin{bmatrix} g_1^{(0)} \\ g_4^{(0)} \end{bmatrix}. \tag{15}$$

Now, it can be easily observed that equations (12) *and* (15) *can be encapsulated into a relation of the form* (9)*, where*

$$\mathbf{F}^{(2)} = \left[\begin{array}{c|c|c} \mathbf{I}_{n_g \times n_g} + \mathbf{Q} \left[\hat{\mathbf{e}}_1 \quad \hat{\mathbf{e}}_4\right]^{\mathrm{T}} & \mathbf{0}_{n_g \times n_d} & \mathbf{0}_{n_g \times n_l} \\ \hline \mathbf{0}_{n_d \times n_g} & \mathbf{I}_{n_d \times n_d} & \mathbf{0}_{n_d \times n_l} \\ \hline \mathbf{H}\mathbf{Q} \left[\hat{\mathbf{e}}_1 \quad \hat{\mathbf{e}}_4\right]^{\mathrm{T}} & \mathbf{0}_{n_l \times n_d} & \mathbf{I}_{n_l \times n_l} \end{array}\right]$$

and $\hat{\mathbf{e}}_1, \hat{\mathbf{e}}_2, \ldots, \hat{\mathbf{e}}_{n_g}$ *denote the standard basis for* $\mathbb{R}^{n_g}$*.*

Example 3 (Islanding)**.** *A contingency may cause islanding, which means the separation of a number of buses from the main network. For example, consider the outage of branches* 3*,* 7 *and* 8*. The notion of GLODF is not well-defined in this case since the removal of the branches* 3*,* 7 *and* 8 *disconnects the network. Instead, this contingency can be modeled as two consecutive contingencies:*

1) *Outage of the loads* 4*,* 8 *and* 9*,*
2) *Outage of the branch* 3*.*

In this case, the post-contingency flows of branches 7 *and* 8 *turn into negligible amounts due to zero injection at buses* 4*,* 8 *and* 9 *(post-contingency flows become zero if no demand is considered at buses* 4*,* 8 *and* 9 *at the point of linearization* $\hat{\mathbf{x}}$*).*

Example 4 (Disconnection)**.** *Consider the outage of the branch* 2 *and suppose that the two disconnected parts of the network must be operated independently after the outage and continue to fulfill the demand. As before, the notion of GLODF is not well-defined in this case and we need to model the outage through a pre-specified proportionality factor matrix* $\mathbf{Q} \in \mathbb{R}^{n_g \times 1}$ *as*

$$\mathbf{g}^{(4)} = \mathbf{g}^{(0)} + \mathbf{Q} \times f_2^{(0)}, \tag{16a}$$

$$\mathbf{f}^{(4)} = \mathbf{f}^{(0)} + \mathbf{H}\mathbf{Q} \times f_2^{(0)}, \tag{16b}$$

where

$$Q_1 + Q_2 + Q_4 + Q_5 = -1 \quad \text{and} \quad Q_3 = 1.$$

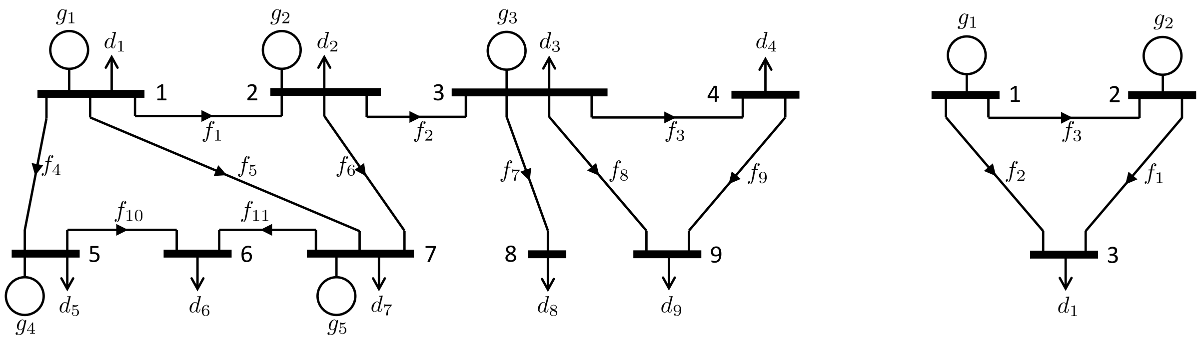

(a) (b)

Fig. 1: (a) The 9-bus network discussed in Examples 1, 2, 3 and 4; (b) the 3-bus network discussed in Example 5.

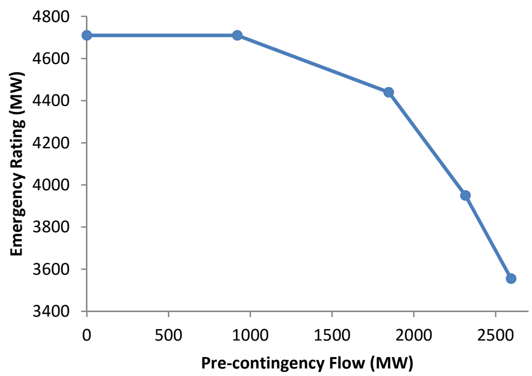

Fig. 2: This figure borrowed from [5] illustrates the variable emergency rating of a transmission line as a function of its pre-contingency flow.

Thus, we have

$$\mathbf{F}^{(4)} = \left[\begin{array}{c:c:c} \mathbf{I}_{n_g \times n_g} & \mathbf{0}_{n_g \times n_d} & \mathbf{Q}\,\tilde{\mathbf{e}}_2^{\mathrm{T}} \\ \hdashline \mathbf{0}_{n_d \times n_g} & \mathbf{I}_{n_d \times n_d} & \mathbf{0}_{n_d \times n_l} \\ \hdashline \mathbf{0}_{n_l \times n_g} & \mathbf{0}_{n_l \times n_d} & \mathbf{I}_{n_l \times n_l} + \mathbf{H}\mathbf{Q}\,\tilde{\mathbf{e}}_2^{\mathrm{T}} \end{array}\right].$$

In this case, the post-contingency flow $f_2^{(4)}$ *becomes zero and the power balance is preserved for each part of the network after the outage.*

In the preventive control mode, contingency $k \in \{1, 2, ..., n_c\}$ can be modeled as the addition/removal of a set of components, namely m contingent components. The corresponding transition matrix $\mathbf{F}^{(k)}$ can be generated according to the formula

$$\mathbf{F}^{(k)} = \mathbf{F}_1 \times \mathbf{F}_2 \times \ldots \times \mathbf{F}_m, \tag{17}$$

where $\mathbf{F}_1, \mathbf{F}_2, \ldots, \mathbf{F}_m$ are the transition matrices associated to the removal/addition of individual contingent components. In most practical corrective control modes, an arbitrary combination of outages and recourse actions that involve lines, generators and loads of the network can also be modeled through the equation (9).

D. Variable Emergency Ratings

In practice, it is often the case that the emergency rating of a line is defined as a piecewise linear concave function with respect to the pre-contingency flow of that line. Figure 2 shows an example of such function, which is borrowed from [5]. Variable emergency ratings for a line $q \in \{1, \ldots, n_l\}$ can be imposed through multiple linear constraints as

$$|f_q^{(k)}| \leq -a_{q,m}^{(k)}|f_q| + u_{q,m}^{(k)}, \tag{18}$$

for every $m \in \{1, \ldots, m_q\}$ and $k \in \{1, \ldots, n_c\}$, where m_q is the number of segments that the rating function is described by, and $\{a_{q,m}^{(k)}\}_{m=1}^{z_q}$ and $\{u_{q,m}^{(k)}\}_{m=1}^{z_q}$ are nonnegative constants. With no loss of generality, we only consider constant ratings in the remainder of this work. Note that our formulation can be revised by introducing additional constraints corresponding to (18) in order to include variable emergency ratings.

E. Safe Operating Region

Definition 1 (Safe operating region)**.** *Define the safe operating region as the set* $\mathcal{S}$ *consisting of all vectors* $\mathbf{x} \in \mathbb{R}^n$ *that satisfy the pre- and post-contingency network constraints:*

$$\mathbf{A}\mathbf{x} = \mathbf{b}, \tag{19a}$$

$$\mathbf{l}^{(k)} \leq \mathbf{F}^{(k)}\mathbf{x} \leq \mathbf{u}^{(k)} \qquad \forall k \in \{0, 1, \ldots, n_c\}. \tag{19b}$$

The number of inequality constraints in (19b) is equal to $2 \times (n_c + 1) \times n$, which can be prohibitive for applications that require solving mixed-integer optimization problems over $\mathcal{S}$. The main objective of this paper is to obtain a minimal subset of constraints among the inequalities in (19b) that are sufficient to characterize the set $\mathcal{S}$.

III. Constraint Screening

In this section, we first derive easy-to-calculate lower and upper bounds for the entries of $\mathbf{x}$, and then exploit the bounds to identify redundant constraints.

A. Accurate Reliable Bounds

In this subsection, we introduce an algorithm for obtaining lower and upper bounds for the entries of $\mathbf{x}$, which is based on solving a set of linear programing (LP) problems. Two LPs need to be solved for each entry of $\mathbf{x}$. Each LP aims to either minimize or maximize one entry of $\mathbf{x}$ subject to a subset of constraints in (19). The main difference between the approach to be developed next and the bound tightening scheme in [16] and [18] is that we exploit the sparse structure of the matrices $\mathbf{F}^{(0)}, \mathbf{F}^{(1)}, \ldots, \mathbf{F}^{(n_c)}$ in order to define each LP based on a small subset of constraints in (19b). This would lead to simple LPs.

To obtain bounds on the network parameters, we adopt the approach proposed in [6] for grouping the security constraints in (19b) and performing cancellation within each group in parallel. This approach includes two partitioning schemes:

1) *Contingency-based partitioning:* The constraints are divided into n_c groups based on their corresponding contingency cases. More precisely, the following group of constraints is considered for every contingency k:
$$l_i^{(k)} \le x_i^{(k)} \le u_i^{(k)}, \quad \forall i \in \{1, \ldots, n\}. \tag{20}$$
2) *Component-based partitioning:* The partitioning of constraints is based on the component associated to each constraint. More precisely, the pre- and post-contingency constraints for the i-th component are all considered in one group as follows:
$$l_i^{(k)} \le x_i^{(k)} \le u_i^{(k)}, \quad \forall k \in \{1, \ldots, n_c\}. \tag{21}$$

By exploiting the above-mentioned partitioning strategies, we develop a method for obtaining lower and upper bounds on the entries of $\mathbf{x}$. For every $i \in \{1, \ldots, n\}$, two LPs are solved to obtain the bounds on x_i, where each LP is subject to only those security constraints in (19b) that either impose a limit on component i or correspond to a contingency case that involves the outage of component i.

Definition 2. *For every $i = 1, 2, \ldots n$, define $\mathcal{R}_i$ as the set of operating points $\mathbf{x} \in \mathbb{R}^n$ that satisfy the relations*
$$\mathbf{A}\mathbf{x} = \mathbf{b}, \tag{22a}$$
$$\mathbf{l} \le \mathbf{x} \le \mathbf{u}, \tag{22b}$$
$$l_j^{(k)} \le \mathbf{e}_j^{\mathrm{T}} \mathbf{F}^{(k)} \mathbf{x} \le u_j^{(k)} \qquad \forall k, j \quad \text{s.t.} \quad F_{ji}^{(k)} \neq 0. \tag{22c}$$

The constraints in (22c) are the collection of those constraints in (19b) that *directly* involve x_i. Note that $\mathcal{S} \subseteq \mathcal{R}_i$. Let $n_{c,i}$ denote the number of contingency cases that involve the outage of component $i \in \{1, \ldots, n\}$. Observe that the number of inequalities in (22c) is less than or equal to
$$2 \times n_{c,i} \times n + 2 \times n_c, \tag{23}$$
which is likely to be much smaller than the total number of security constraints (i.e., $2 \times n_c \times n$) for real-world systems. Notice that the first term in (23) represents the number of constraints associated with those contingencies that involve the outage of component i, whereas the second term accounts for the number of constraints that impose limits on one of the quantities $x_i^{(1)}, \ldots, x_i^{(n_c)}$.

Definition 3 (Reliable bounds)**.** *For every $i = 1, 2, \ldots, n$, define*
$$l_i^{\mathrm{rel}} \triangleq \min\{x_i | \mathbf{x} \in \mathcal{R}_i\} \ \text{ and } \ u_i^{\mathrm{rel}} \triangleq \max\{x_i | \mathbf{x} \in \mathcal{R}_i\} \tag{24}$$
as the accurate reliable lower and upper bounds for x_i. Moreover, define $\mathbf{l}^{\mathrm{rel}} \triangleq [l_i^{\mathrm{rel}}]_{i=1}^n$ and $\mathbf{u}^{\mathrm{rel}} \triangleq [u_i^{\mathrm{rel}}]_{i=1}^n$ as the vectors of accurate reliable lower and upper bounds.

The accurate reliable bounds defined in (24) can be found efficiently by solving $2n$ linear programs in parallel, where each involves a modest number of constraints. In order to elaborate on the definition of accurate reliable bounds, a simple example will be provided below.

Example 5. *Consider two contingency cases for the 3-bus network shown in Figure 1(b), where the first case involves the single outage of generator 2 and the second case involves the single outage of line 1. The vector*
$$\mathbf{x} = [g_1 \quad g_2 \quad d_1 \quad f_1 \quad f_2 \quad f_3]^{\mathrm{T}}$$
describes the base case state of the system, where g_1 and g_2 denote the active power values produced by generators 1 and 2, d_1 is the amount of power consumed by the single load in the system at bus 3, and f_i denotes the amount of power transmitted through the line i of the network for $i = 1, 2, 3$. In addition, the post-contingency state vectors can be obtained as follows:
$$\mathbf{x}^{(1)} = [g_1^{(1)} \quad g_2^{(1)} \quad d_1^{(1)} \quad f_1^{(1)} \quad f_2^{(1)} \quad f_3^{(1)}]^{\mathrm{T}},$$
$$\mathbf{x}^{(2)} = [g_1^{(2)} \quad g_2^{(2)} \quad d_1^{(2)} \quad f_1^{(2)} \quad f_2^{(2)} \quad f_3^{(2)}]^{\mathrm{T}}.$$
In order to ensure a secure operation, lower and upper bounds should be imposed on the parameters of each component at every operating scenario. Thus, according to (19)*, the safe operating region for the network can be described using $2 \times n \times (n_c + 1) = 36$ inequalities.*

In order to calculate the accurate reliable lower and upper bounds for line 1, we need to perform two optimization problems over the set $\mathcal{R}_4$ (since f_1 is represented by the 4^{th} entry of $\mathbf{x}$). According to Definition 2, the set $\mathcal{R}_4$ is described by the inequalities
$$l_4^{(k)} \le f_1^{(k)} \le u_4^{(k)}, \qquad \forall k \in \{1, 2\} \tag{25a}$$
$$l_1^{(2)} \le g_1^{(2)} \le u_1^{(2)}, \qquad l_2^{(2)} \le g_2^{(2)} \le u_2^{(2)}, \tag{25b}$$
$$l_5^{(2)} \le f_2^{(2)} \le u_5^{(2)}, \qquad l_6^{(2)} \le f_3^{(2)} \le u_6^{(2)}, \tag{25c}$$
$$l_3^{(2)} \le d_1^{(2)} \le u_3^{(2)}, \tag{25d}$$
in addition to (22a) *and* (22b)*. The basic idea behind the definition of $\mathcal{R}_4$ is that we only consider those security inequalities that directly involve f_1 (see* (22c)*). For example, the constraints in* (25a) *represent all of the post-contingency limits on line 1, and they directly involve f_1 due to the equations*
$$f_1^{(1)} = f_1 + F_{4,2}^{(1)} \times g_2, \tag{26}$$
$$f_1^{(2)} = F_{4,4}^{(2)} \times f_1. \tag{27}$$
Likewise, the remaining constraints in (25) *involve f_1 because they correspond to the outage of line 1.*

B. Computationally Cheap Reliable Bounds

As an alternative to the method proposed above, a computationally cheap approach can be adopted for obtaining reliable bounds. This method obviates the need for solving optimization problems [19].

For every $\mathbf{x} \in \mathcal{S}$, $j \in \{1, \dots, n\}$ and $k \in \{0, 1, \dots, n_c\}$, we have

$$l_j^{(k)} \le \sum_{\ell=1}^{n} F_{j\ell}^{(k)} x_\ell \le u_j^{(k)}. \tag{28}$$

Assuming that $F_{ji}^{(k)} > 0$ for an index $i \in \{1, \dots, n\}$, the following bounds can be derived for x_i:

$$x_i \le \frac{1}{F_{ji}^{(k)}} \left(u_j^{(k)} - \sum_{\ell \ne i} F_{j\ell}^{(k)} v_{\ell j}^{(k)} \right) \tag{29a}$$

$$x_i \ge \frac{1}{F_{ji}^{(k)}} \left(l_j^{(k)} - \sum_{\ell \ne i} F_{j\ell}^{(k)} w_{\ell j}^{(k)} \right) \tag{29b}$$

where

$$v_{\ell j}^{(k)} \triangleq l_\ell \, \mathcal{I}_{F_{j\ell}^{(k)} > 0} + u_\ell \, \mathcal{I}_{F_{j\ell}^{(k)} < 0} \tag{30a}$$

$$w_{\ell j}^{(k)} \triangleq l_\ell \, \mathcal{I}_{F_{j\ell}^{(k)} < 0} + u_\ell \, \mathcal{I}_{F_{j\ell}^{(k)} > 0} \tag{30b}$$

If $F_{ji}^{(k)} < 0$, two bounds similarly to (29) can also be obtained for x_i. Then, the tightest upper and lower bounds can be chosen by searching through all pairs $(j,k) \in \{1, \dots, n\} \times \{0, 1, \dots, n_c\}$. We refer to the bounds obtained through this procedure as computationally cheap reliable bounds for x_i.

Unlike accurate reliable bounds that require solving linear programs, the vectors of computationally cheap reliable bounds can be readily calculated through simple formulas. For example, these bounds are found within one minute for large systems such as the ERCOT 5506-bus system, using a laptop computer with an Intel Core i7 quad-core 2.20 GHz CPU and 12GB RAM.

C. Constraint Screening Algorithm

The inequalities

$$\mathbf{l}^{\text{rel}} \le \mathbf{x} \le \mathbf{u}^{\text{rel}}, \quad \forall \mathbf{x} \in \mathcal{S} \tag{31}$$

can be used to eliminate some of the redundant scalar constraints in (19) through an interval arithmetic procedure [20]. The *constraint screening algorithm* provided in this section formalizes this procedure. The outputs of the algorithm are two sets $\mathcal{A}^+, \mathcal{A}^- \subseteq \{1, \dots, n\} \times \{0, 1, \dots, n_c\}$ with the property that

$$\mathcal{S} = \left\{ \mathbf{x} \;\middle|\; \begin{array}{ll} \mathbf{e}_i^{\mathrm{T}} \mathbf{F}^{(k)} \mathbf{x} \le u_i^{(k)} & (i,k) \in \mathcal{A}^+, \\ \mathbf{e}_i^{\mathrm{T}} \mathbf{F}^{(k)} \mathbf{x} \ge l_i^{(k)} & (i,k) \in \mathcal{A}^- \end{array} \right\}. \tag{32}$$

In other words, the statement $(i,k) \notin \mathcal{A}^+$ means that the constraint $x_i^{(k)} \le u_i^{(k)}$ is declared redundant and the statement $(i,k) \notin \mathcal{A}^-$ means that the constraint $x_i^{(k)} \ge l_i^{(k)}$ is declared redundant by the algorithm.

Algorithm 1 Constraint screening algorithm

Require: $\mathbf{l}^{\text{rel}} \in (\{-\infty\} \cup \mathbb{R})^n$ and $\mathbf{u}^{\text{rel}} \in (\mathbb{R} \cup \{\infty\})^n$

1: $\mathcal{A}^+ \leftarrow \{1, \dots, n\} \times \{0, 1, \dots, n_c\}$
2: $\mathcal{A}^- \leftarrow \{1, \dots, n\} \times \{0, 1, \dots, n_c\}$
3: **for** $k = 0, 1 \dots, n_c$ **do**
4: $\quad \mathbf{L}^{(k)} := \left[l_i^{\text{rel}} \mathcal{I}_{F_{ji}^{(k)} > 0} + u_i^{\text{rel}} \mathcal{I}_{F_{ji}^{(k)} < 0} \right]_{i,j=1,\dots,n}$
5: $\quad \mathbf{U}^{(k)} := \left[l_i^{\text{rel}} \mathcal{I}_{F_{ji}^{(k)} < 0} + u_i^{\text{rel}} \mathcal{I}_{F_{ji}^{(k)} > 0} \right]_{i,j=1,\dots,n}$
6: $\quad \tilde{\mathbf{l}}^{(k)} := \mathrm{diag}\{\mathbf{F}^{(k)} \mathbf{L}^{(k)}\}$
7: $\quad \tilde{\mathbf{u}}^{(k)} := \mathrm{diag}\{\mathbf{F}^{(k)} \mathbf{U}^{(k)}\}$
8: $\quad$ **for** $i = 1 \dots, n$ **do**
9: $\quad\quad$ **if** $l_i^{(k)} < \tilde{l}_i^{(k)}$ **then**
10: $\quad\quad\quad \mathcal{A}^+ \leftarrow \mathcal{A}^+ \setminus \{(i,k)\}$
11: $\quad\quad$ **end if**
12: $\quad\quad$ **if** $\tilde{u}_i^{(k)} < u_i^{(k)}$ **then**
13: $\quad\quad\quad \mathcal{A}^- \leftarrow \mathcal{A}^- \setminus \{(i,k)\}$
14: $\quad\quad$ **end if**
15: $\quad$ **end for**
16: **end for**

Theorem 1. *Suppose that $\mathcal{A}^+$ and $\mathcal{A}^-$ are the outputs of the constraint screening algorithm. Then, the constraints in* (19b) *that correspond to the members of $\mathcal{A}^+$ and $\mathcal{A}^-$ are sufficient for describing the safe operating region $\mathcal{S}$ and the remaining inequality constraints in* (19b) *are redundant.*

Proof. According to Steps 6 and 7 of the algorithm, define

$$\tilde{\mathbf{l}}^{(k)} \triangleq \mathrm{diag}\{\mathbf{F}^{(k)} \mathbf{L}^{(k)}\} \quad \text{and} \quad \tilde{\mathbf{u}}^{(k)} \triangleq \mathrm{diag}\{\mathbf{F}^{(k)} \mathbf{U}^{(k)}\}.$$

To prove the theorem, it suffices to show that

$$\tilde{\mathbf{l}}^{(k)} \le \mathbf{x}^{(k)} \le \tilde{\mathbf{u}}^{(k)} \tag{33}$$

for every $\mathbf{x}^{(k)} = \mathbf{F}^{(k)} \mathbf{x}$, where $\mathbf{x}$ is a member of $\mathcal{S}$. To this end, one can write:

$$\begin{aligned} \mathbf{x} \in \mathcal{S} \;&\Rightarrow\; l_i^{\text{rel}} \le x_i \le u_i^{\text{rel}}, & \forall i = 1, \dots, n \\ &\Rightarrow\; F_{ji} L_{ij}^{(k)} \le F_{ji} x_i \le F_{ji} U_{ij}^{(k)}, & \forall i = 1, \dots, n \\ &\Rightarrow\; \sum_{i=1}^{n} F_{ji} L_{ij}^{(k)} \le \sum_{i=1}^{n} F_{ji} x_i \le \sum_{i=1}^{n} F_{ji} U_{ij}^{(k)} & \\ &\overset{(9)}{\Rightarrow}\; \tilde{l}_j^{(k)} \le x_j^{(k)} \le \tilde{u}_j^{(k)}. & \end{aligned} \tag{34}$$

The two inequalities in (34) imply the following: (i) if $l_i^{(k)} < \tilde{l}_i^{(k)}$, then the constraint $l_i^{(k)} \le x_i^{(k)}$ in (19b) can be declared redundant, (ii) if $\tilde{u}_i^{(k)} < u_i^{(k)}$, then $x_i^{(k)} \le u_i^{(k)}$ can be declared redundant. $\square$

As will be shown in Section IV, a vast majority of redundant constraints are identified by means of the constraint screening algorithm for several real-world systems.

D. Exhaustive Search

The proposed constraint screening algorithm reduces the set of inequalities required for the characterization of $\mathcal{S}$, but it does not necessarily yield a minimal set. To further reduce the

Test cases	Ratio of post to pre-fault ratings of regular lines	Number of special lines	Ratio for special lines
Polish 2383wp	1.3	15	1.5
Polish 2736sp	1.2	21	4.0
Polish 2737sop	1.05	17	3.1
Polish 2746wop	1.05	21	2.0
Polish 2746wp	1.3	19	3.1
Polish 3012wp	1.5	0	1.5
Polish 3120sp	1.5	15	1.95
Polish 3375wp	1.3	13	1.5
PEGASE 1354	1.3	30	2.9
PEGASE 2869	1.3	21	2.5
ERCOT 5506	1.3	28	1.8

TABLE I: Description of the considered emergency ratings.

size of the set, an exhaustive search algorithm can be deployed. Consider the optimization problem

$$\underset{\mathbf{x}\in\mathbb{R}^n}{\text{minimize}} \quad \mathbf{c}^{\mathrm{T}}\mathbf{x} \tag{35a}$$

$$\text{subject to} \quad \lambda_i^{(k)}: \ \mathbf{e}_i^{\mathrm{T}}\mathbf{F}^{(k)}\mathbf{x} \leq u_i^{(k)}, \quad \forall (i,k)\in\mathcal{A}^{+} \tag{35b}$$

$$\gamma_i^{(k)}: \ \mathbf{e}_i^{\mathrm{T}}\mathbf{F}^{(k)}\mathbf{x} \geq l_i^{(k)}, \quad \forall (i,k)\in\mathcal{A}^{-} \tag{35c}$$

for some constant vector $\mathbf{c}$, where $\lambda_i^{(k)} \geq 0$ and $\gamma_i^{(k)} \leq 0$ denote the Lagrange multipliers for the corresponding constraints. One can identify all of the redundant constraints in (32) by solving a sequence of optimization problems of the form (35) by choosing $\mathbf{c}^{\mathrm{T}}\mathbf{x}$ as

$$\mathbf{c}^{\mathrm{T}}\mathbf{x} = \mathbf{e}_i^{\mathrm{T}}\mathbf{F}^{(k)}\mathbf{x} \tag{36}$$

for every pair $(i,k)\in\mathcal{A}^{-}$ and

$$\mathbf{c}^{\mathrm{T}}\mathbf{x} = -\mathbf{e}_i^{\mathrm{T}}\mathbf{F}^{(k)}\mathbf{x} \tag{37}$$

for every pair $(i,k)\in\mathcal{A}^{+}$. If the optimal objective value does not reach the minimum value imposed by

$$l_i^{(k)} \leq \mathbf{e}_i^{\mathrm{T}}\mathbf{F}^{(k)}\mathbf{x} \leq u_i^{(k)}, \tag{38}$$

then the corresponding constraint can be declared redundant. In addition, every nonzero Lagrange multipliers certifies that its corresponding constraint is not redundant and contributes to the definition of $\mathcal{S}$.

IV. Simulation Results

In order to evaluate the performance of the proposed constraint screening algorithm, we aim to conduct extensive simulations on Polish networks [28], Pan European Grid Advanced Simulation and State Estimation (PEGASE) [29], and Electric Reliability Council of Texas (ERCOT) data for planning. The simulations are run on a laptop computer with an Intel Core i7 quad-core 2.20 GHz CPU and 12GB RAM. The computation times reported in this section are for a serial implementation in MATLAB and the decoupled LPs for finding the reliable bounds are not solved in parallel. In all of the simulations, the constraint redundancy test is applied to a single time slot of the SCUC problem (because the proposed algorithm works on different time instances of the problem independently). Moreover, it is assumed that the total cost function (including generation, startup and showdown costs) and the on/off status of each generator are unknown. To account for this condition, we impose the lower bound $\min\{0, g_s^{\min}\}$ on g_s for every generator $s\in\{1,\ldots,n_g\}$, where $g_s^{\min}$ is the minimum output of generator s when it is active.

According to the modeling discussed in Example 2, for every post-contingency scenario that involves a power imbalance, the amount of mismatch is compensated by in-service generators proportional to their maximum capacity. Moreover, according to Example 3, every disconnected load and generator is treated as a contingent component in case of islanding. First, the topology of post-contingent networks corresponding to all cases is analyzed in order to diagnose islanding and then the matrices $\mathbf{F}^{(0)}, \mathbf{F}^{(1)}, \ldots, \mathbf{F}^{(n_c)}$ are generated accordingly. The run time of this process does not exceed 2 minutes for each of the test systems to be analyzed next. In what follows, three experiments will be conducted to evaluate the performance of the proposed method under different conditions.

Experiment 1. Assume that the exact value of each load is known and that the single outage of each line and generator is considered as a contingency. We consider synthetic emergency ratings that are obtained by solving a power flow problem for the base case and examining the resulting post-contingency flows. For each system, a number of lines whose post-contingency flows are significantly higher than their normal ratings for at least one of the contingency cases are labeled as *special lines*. The emergency ratings for special lines are set as up to 4 times larger than their normal ratings, while this ratio is up to 1.5 for all other lines. Table I shows the ratios and the number of special lines for each test case. Each ratio is chosen through trial and error and is not more than 10% distanced from the minimum amount that is necessary to assure the feasibility of the security problem. We have observed that the performance of the proposed algorithm is not sensitive to the choice of these ratios.

The results for Experiment 1 are summarized in Table II. The third column indicates the total number of line flow constraints for all pre- and post-contingency cases. The computationally cheap and accurate reliable bounds are calculated independently for every test case. The forth and fifth columns show the numbers of branch flow constraints remained after using the constraint screening through the computationally cheap and accurate reliable bounds, respectively. Figures 3 and 4 depict comparative histograms of differences between the upper and lower limits on line flows obtained by the accurate and computationally cheap reliable bounds for the ERCOT system.

The sixth column of Table II shows the run time (in minutes) for obtaining the accurate reliable bounds without parallel processing. For each test system, the computationally cheap reliable bounds are derived in less than 2 minutes. After calculating the reliable bounds, the run time of the screening algorithm is less than 30 seconds for all of the cases. For each test case, we have also obtained a minimal set of inequality constraints on branch flows that describes the set $\mathcal{S}$. The minimal set for each case is obtained by running the exhaustive search procedure explained in Section III on the

Test cases	Number of contingencies	Total num. of line inequality constraints	Num. of undominated line constraints after screening through comp. cheap bounds	Num. of undominated line constraints after screening through accurate bounds	Comp. time for obtaining accurate bounds	Size of the minimal set of line constraints	Running time of exhaustive search
Polish 2383wp	3,223	18,673,408	46,995	329	48 m	70	2 m
Polish 2736sp	3,539	23,144,520	97,998	101	66 m	15	2 m
Polish 2737sop	3,488	22,811,082	150,492	101	66 m	14	2 m
Polish 2746wop	3,738	24,729,746	194,210	5,135	78 m	22	78 m
Polish 2746wp	3,735	24,500,688	62,535	69	84 m	14	1 m
Polish 3012wp	3,959	28,275,952	89,532	139	162 m	59	2 m
Polish 3120sp	3,991	29,484,912	149,561	4,172	174 m	79	126 m
Polish 3375wp	4,640	38,622,402	566,492	10,048	198 m	119	258 m
PEGASE 1354	2,251	6,449,728	15,408	1,652	30 m	259	12 m
PEGASE 2869	5,092	27,940,198	56,369	3,689	186 m	426	106 m
ERCOT 5506	7,120	91,675,754	74,721	827	258 m	100	36 m

TABLE II: The performance of the constraint screening algorithm followed by an exhaustive search for Polish, PEGASE and ERCOT systems.

Test cases	Num. of undominated line constraints after screening through comp. cheap bounds	Num. of undominated line constraints after screening through accurate bounds	Size of the minimal set of line constraints
Polish 2383wp	176,453	1,951	312
Polish 2736sp	571,468	560	88
Polish 2737sop	701,546	789	57
Polish 2746wop	1,197,428	29,523	79
Polish 2746wp	442,135	448	83
Polish 3012wp	289,754	941	183
Polish 3120sp	798,094	33,507	216
Polish 3375wp	1,846,460	47,829	340
PEGASE 1354	132,819	11,867	418
PEGASE 2869	238,962	26,190	1,768
ERCOT 5506	289,251	2,148	267

TABLE III: The performance of the constraint screening algorithm followed by an exhaustive search for Polish, PEGASE and ERCOT systems, with $\pm 10\%$ load uncertainty.

Test cases	Total num. of line inequality constraints	Num. of undominated line constraints after screening through comp. cheap bounds	Num. of undominated line constraints after screening through accurate bounds	Size of the minimal set of line constraints
Polish 2383wp	11,589,792	23,313	816	128
Polish 2736sp	14,023,008	14,987	735	174
Polish 2737sop	14,031,012	16,079	294	65
Polish 2746wop	14,063,028	31,912	3,490	98
Polish 2746wp	14,063,028	17,782	2,142	188
Polish 3012wp	14,295,144	6,161	540	74
Polish 3120sp	14,779,386	16,838	1,490	91
Polish 3375wp	16,652,322	84,544	10,641	361
PEGASE 1354	7,967,982	31,833	4,259	168
PEGASE 2869	18,337,164	52,200	8,519	2,059
ERCOT 5506	26,681,334	22,037	6,026	467

TABLE IV: The performance of the constraint screening algorithm followed by an exhaustive search for Polish, PEGASE and ERCOT systems, with $\pm 10\%$ load uncertainty and random contingencies.

set of undominated line constraints after screening through the accurate bounds. In other words, the computationally cheap bounds are not used for obtaining the minimal set in our simulations. The sizes of these minimal sets are shown in the seventh column of Table II, and the run time of the exhaustive search is also shown in the last column.

In summary, the minimum number of constraints provided in the seventh column of Table II is obtained by the following sequence of actions:

1) Topology analysis of post-contingency networks and calculation of the matrices $\mathbf{F}^{(0)}, \mathbf{F}^{(1)}, \ldots, \mathbf{F}^{(n_c)}$
2) Calculation of the accurate reliable bounds explained in Section III-A
3) Running the constraint screening algorithm explained in Section III-C, using the accurate reliable bounds
4) The exhaustive search algorithm from Section III-D.

Note that solvers such as CPLEX have generic preprocessors for removing redundant constraints. However, the number of security constraints in most of our simulations is so large that such solvers may run out of memory or fail to remove all redundant constraints. In contrast, the method proposed in this work is tailored to eliminating the redundant constraints by exploiting key features of the SCUC problem.

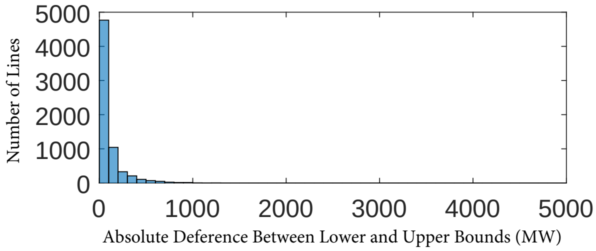

Fig. 3: Histogram of absolute differences between the accurate lower and upper reliable bounds on line flows for the ERCOT system.

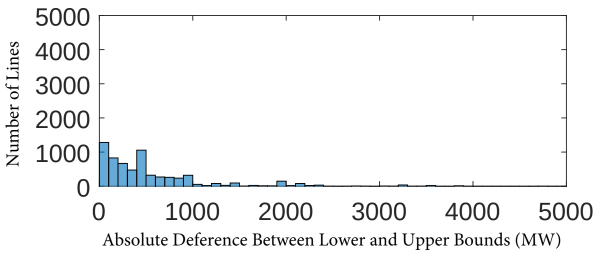

Fig. 4: Histogram of absolute differences between the computationally cheap lower and upper reliable bounds on line flows for the ERCOT system.

Experiment 2. This is built upon Experiment 1 by considering a $\pm 10\%$ demand uncertainty. The main motivation is to test the effectiveness of the proposed method under uncertainty. It is aimed to demonstrate that the constraint screening can be performed well before solving the SCUC problem if the load prediction errors are known. All loads are assumed to be unknown but away from their forecasts by at most 10%. As before, emergency ratings are defined the same way as in Experiment 1, and every single outage of lines and generators is considered as a contingency. The results are shown in Table III.

Experiment 3. Consider the previous experiment with a $\pm 10\%$ demand uncertainty, but assume that the set of contingencies consists of 2000 randomly generated cases where each may involve the outage of multiple components. Experiment 3 is conducted in order to test the effectiveness of the proposed method for contingency cases of day-ahead SCUC problems that involve multiple components simultaneously. The emergency ratings for this experiment are up to 4 times larger than their normal ratings in order to assure feasibility. The following definition is necessary to explain the procedure for constructing contingencies: a generator is adjacent to a line if it belongs to one of its ends, two generators are adjacent if they belong to the same node, and two lines are adjacent if they share a node.

The set of contingent components $\mathcal{C}_k$ for each scenario $k \in \{1, \dots, n_c\}$ is randomly constructed through the following procedure:

1) Initiate $\mathcal{C} := \{c_0\}$, where c_0 is a uniformly chosen line or generator.
2) Stop with probability 0.7; otherwise, uniformly choose a line or generator $c' \notin \mathcal{C}$ that is adjacent to one of the members of $\mathcal{C}$ and set $\mathcal{C} := \mathcal{C} \cup \{c'\}$.
3) Go back to Step 2.

The results for this experiment are shown in Table IV.

V. Conclusions

This paper studies the problem of screening redundant security constraints for the safe operation of power grids. The objective is to design a cheap, parallelizable computational method that is able to find a minimal subset of security constraints whose satisfaction is necessary and sufficient for the satisfaction of all security constraints. The minimal subset to be found is independent of the unknown unit commitment parameters and uncertain load values. Instead, it mainly depends on the network topology, the lower and upper bounds on nodal power injections and the line flow ratings. The proposed method involves solving a number of linear programs in parallel. This algorithm can be utilized to obtain a small set of potentially binding constraints prior to solving the security-constrained unit commitment (SCUC) problem, and it serves as a mechanism for finding a reduced-order model of security constraints. Our simulations on real-world data verify that the proposed algorithm is able to eliminate millions of redundant constraints, leading to reduced-order models with only a few hundred security constraints. The computational method developed in this work analyzes the security constraints of the problem that are modeled as linear inequalities with respect to the base-case parameters.

References

[1] F. F. Wu, K. Moslehi, and A. Bose, "Power system control centers: Past, present, and future," *Proceedings of the IEEE*, vol. 93, no. 11, pp. 1890–1908, 2005.

[2] J. Salmeron, K. Wood, and R. Baldick, "Analysis of electric grid security under terrorist threat," *IEEE Transactions on Power Systems*, vol. 19, no. 2, pp. 905–912, May 2004.

[3] B. Liscouski and W. Elliot, "Final report on the August 14, 2003 blackout in the United States and Canada: Causes and recommendations," *A report to US Department of Energy*, vol. 40, no. 4, 2004.

[4] S. Srivastava, A. Velayutham, K. Agrawal, and A. Bakshi, "Report of the enquiry committee on grid disturbance in northern region on 30th July 2012 and in northern, eastern & north-eastern region on 31st July, 2012."

[5] P. Peng, S. Chang, and J. Dyer, "Inclusion of post-contingency actions in security constrained scheduling," *Atlanta, GA, USA: ABB/VENTYX http://www.ferc.gov/CalendarFiles/20140411131928-T4-B%20-%20Peng.pdf*.

[6] A. J. Ardakani and F. Bouffard, "Identification of umbrella constraints in DC-based security-constrained optimal power flow," *IEEE Transactions on Power Systems*, vol. 28, no. 4, pp. 3924–3934, 2013.

[7] V. Brandwajn, "Efficient bounding method for linear contingency analysis," *IEEE Transactions on Power Systems*, vol. 3, no. 1, pp. 38–43, 1988.

[8] V. Brandwajn and M. Lauby, "Complete bounding method for AC contingency screening," *IEEE Transactions on Power Systems*, vol. 4, no. 2, pp. 724–729, 1989.

[9] Q. Zhai, X. Guan, J. Cheng, and H. Wu, "Fast identification of inactive security constraints in SCUC problems," *IEEE Transactions on Power Systems*, vol. 25, no. 4, pp. 1946–1954, 2010.

[10] B. Hua, Z. Bie, C. Liu, G. Li, and X. Wang, "Eliminating redundant line flow constraints in composite system reliability evaluation," *IEEE Transactions on Power Systems*, vol. 28, no. 3, pp. 3490–3498, 2013.

[11] Y. Fu, Z. Li, and L. Wu, "Modeling and solution of the large-scale security-constrained unit commitment," *IEEE Transactions on Power Systems*, vol. 28, no. 4, pp. 3524–3533, 2013.

[12] Y. Yu, P. B. Luh, E. Litvinov, T. Zheng, J. Zhao, and F. Zhao, "Transmission contingency-constrained unit commitment with uncertain wind generation via interval optimization," in *2015 IEEE Power & Energy Society General Meeting*. IEEE, 2015, pp. 1–5.
[13] X. Ma, D. Sun, and A. Ott, "Implementation of the PJM financial transmission rights auction market system," in *Power Engineering Society Summer Meeting*, vol. 3. IEEE, 2002, pp. 1360–1365.
[14] R. E. Moore, F. Bierbaum, and K.-P. Schwiertz, *Methods and applications of interval analysis*. SIAM, 1979, vol. 2.
[15] J. Hooker, *Logic-based methods for optimization: combining optimization and constraint satisfaction*. John Wiley & Sons, 2011, vol. 2.
[16] H. S. Ryoo and N. V. Sahinidis, "A branch-and-reduce approach to global optimization," *Journal of Global Optimization*, vol. 8, no. 2, pp. 107–138, 1996.
[17] N. V. Sahinidis, "Global optimization and constraint satisfaction: The branch-and-reduce approach," in *Global Optimization and Constraint Satisfaction*. Springer, 2002, pp. 1–16.
[18] A. M. Gleixner, "Exact and fast algorithms for mixed-integer nonlinear programming," 2015.
[19] G. Gamrath, T. Koch, A. Martin, M. Miltenberger, and D. Weninger, "Progress in presolving for mixed integer programming," *Mathematical Programming Computation*, vol. 7, no. 4, pp. 367–398, 2015.
[20] A. Brearley, G. Mitra, and H. P. Williams, "Analysis of mathematical programming problems prior to applying the simplex algorithm," *Mathematical programming*, vol. 8, no. 1, pp. 54–83, 1975.
[21] Z. Wang and F. L. Alvarado, "Interval arithmetic in power flow analysis," *IEEE Transactions on Power Systems*, vol. 7, no. 3, pp. 1341–1349, 1992.
[22] H. Ye and Z. Li, "Necessary conditions of line congestions in uncertainty accommodation," *IEEE Transactions on Power Systems*, vol. PP, no. 99, pp. 1–2, 2015.
[23] Y. Wang, Q. Xia, and C. Kang, "Unit commitment with volatile node injections by using interval optimization," *IEEE Transactions on Power Systems*, vol. 26, no. 3, pp. 1705–1713, 2011.
[24] A. Ardakani and F. Bouffard, "Acceleration of umbrella constraint discovery in generation scheduling problems," *IEEE Transactions on Power Systems*, vol. 30, no. 4, pp. 2100–2109, July 2015.
[25] A. I. Cohen, V. Brandwahjn, and S.-K. Chang, "Security constrained unit commitment for open markets," in *Power Industry Computer Applications, 1999. PICA'99. Proceedings of the 21st 1999 IEEE International Conference*. IEEE, 1999, pp. 39–44.
[26] A. J. Wood and B. F. Wollenberg, *Power generation, operation, and control*. John Wiley & Sons, 2012.
[27] T. Guler, G. Gross, and M. Liu, "Generalized line outage distribution factors," *IEEE Transactions on Power Systems*, vol. 22, no. 2, pp. 879–881, May 2007.
[28] R. D. Zimmerman, C. E. Murillo-Sánchez, and R. J. Thomas, "MATPOWER: Steady-state operations, planning, and analysis tools for power systems research and education," *IEEE Transactions on Power Systems*, vol. 26, no. 1, pp. 12–19, 2011.
[29] S. Fliscounakis, P. Panciatici, F. Capitanescu, and L. Wehenkel, "Contingency ranking with respect to overloads in very large power systems taking into account uncertainty, preventive, and corrective actions," *IEEE Transactions on Power Systems*, vol. 28, no. 4, pp. 4909–4917, 2013.

Ramtin Madani is an Assistant Professor at the Electrical Engineering Department of the University of Texas at Arlington. He received the Ph.D. degree in Electrical Engineering from Columbia University in 2015, and was a postdoctoral scholar in the Department of Industrial Engineering and Operations Research at University of California, Berkeley in 2016.

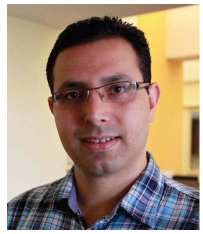

Javad Lavaei is an Assistant Professor in the Department of Industrial Engineering and Operations Research at University of California, Berkeley. He obtained his Ph.D. degree in Computing and Mathematical Sciences from California Institute of Technology in 2011. He has won multiple awards, including NSF CAREER Award, Office of Naval Research Young Investigator Award, DARPA Young Faculty Award, Google Faculty Research Award, Donald P. Eckman Award, Resonate Award, and INFORMS Optimization Society Prize for Young Researchers.

Ross Baldick (F07) received the B.Sc. degree in mathematics and physics and the B.E. degree in electrical engineering from the University of Sydney, Sydney, Australia, and the M.S. and Ph.D. degrees in electrical engineering and computer sciences from the University of California, Berkeley, in 1988 and 1990, respectively. From 1991 to 1992, he was a Post-Doctoral Fellow with the Lawrence Berkeley Laboratory, Berkeley, CA. In 1992 and 1993, he was an Assistant Professor with the Worcester Polytechnic Institute, Worcester, MA. He is currently a Professor with the Department of Electrical and Computer Engineering, University of Texas, Austin.